

Multi-Knowledge Fusion for New Feature Generation in Generalized Zero-Shot Learning

Hongxin Xiang[†], Cheng Xie^{†,§}, *Member, IEEE*, Ting Zeng, and Yun Yang[§], *Member, IEEE*

Abstract—Suffering from the semantic insufficiency and domain-shift problems, most of existing state-of-the-art methods fail to achieve satisfactory results for Zero-Shot Learning (ZSL). In order to alleviate these problems, we propose a novel generative ZSL method to learn more generalized features from multi-knowledge with continuously generated new semantics in semantic-to-visual embedding. In our approach, the proposed Multi-Knowledge Fusion Network (MKFNet) takes different semantic features from multi-knowledge as input, which enables more relevant semantic features to be trained for semantic-to-visual embedding, and finally generates more generalized visual features by adaptively fusing visual features from different knowledge domain. The proposed New Feature Generator (NFG) with adaptive genetic strategy is used to enrich semantic information on the one hand, and on the other hand it greatly improves the intersection of visual feature generated by MKFNet and unseen visual features. Empirically, we show that our approach can achieve significantly better performance compared to existing state-of-the-art methods on a large number of benchmarks for several ZSL tasks, including traditional ZSL, generalized ZSL and zero-shot retrieval.

Index Terms—Image Classification, Zero-Shot Learning, Generative Adversarial Networks, Knowledge Engineering.

I. INTRODUCTION

WITH the renaissance of deep learning, various computer vision tasks have made huge breakthroughs [1], [2], [3]. However, deep learning technology often relies on a large amount of labeled category data, which constitutes a serious bottleneck for building a comprehensive model for the real visual world. In order to overcome this limitation, Zero-Shot Learning (ZSL) [4], [5], [6], [7], [8] was proposed to build such a learning system that can predict new categories that have not been seen in the training phase. In recent years, ZSL has attracted a lot of attention due to its potential to address unseen data in the test stage.

In Zero-Shot Learning (ZSL) classification task, the model needs to identify unseen classes that never appeared in the training phase. This harsh and realistic scene is painful for traditional classification methods because there are no labeled visual data to support the training of unseen classes. In order to solve this problem, most of the existing methods use transfer learning methods, that is, assuming that the model trained on the seen class can be applied to the unseen class, and focus on learning a transferable model. The generative zero-shot learning is one of these methods.

All the authors are with National Pilot School of Software, Yunnan University, Kunming, 650504, China.

[†]Hongxin Xiang and Cheng Xie contributed equally to this work.

[§]Yun Yang (Email: yangyan19@hotmail.com) and Cheng Xie (Email: xiecheng@ynu.edu.cn) are the corresponding authors.

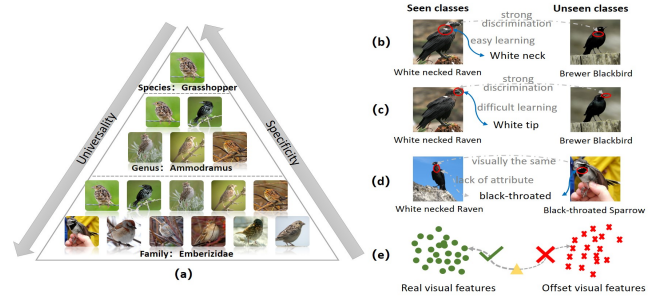


Fig. 1. (a) Multi-knowledge hierarchical structure of Family, Genus and Species, which is an example on the CUB dataset. The relationship of different knowledge is Family>Genus>Species, whose generality and specificity decrease and increase respectively. (b) An example of an attribute with strong discrimination and easy learning, which shows that White neck is important attribute to distinguish White necked Raven from Brewer Blackbird. (c) An example of an attribute with strong discrimination but difficult learning, which shows that White tip is a important attribute to distinguish White necked Raven from Brewer Blackbird but it is difficult to learn the mapping from White tip to the corresponding vision due to visually not obvious. (d) An example of exists visually but not semantically, which shows that the attribute black-throated exists visually in both the seen class White necked Raven and the unseen class Black-throated Sparrow, but the semantics does not exist in the seen class. (e) An example of limiting the generation of visual samples, which shows that when the generated samples are close to the corresponding clusters, they should deviate from those offset visual samples.

The goal of generative zero-shot learning is to establish a semantic-to-visual mapping, and train a classification model that recognizes unseen classes by using synthesized-visual features transformed from unseen classes’ semantics. However, for almost all semantic-to-visual feature learning methods, they still face two major challenges:

1) *The Semantic Insufficiency Challenge*: We often use semantic-visual embedding, including embedding from semantic space to visual space [9], [10], [11], [12] or vice versa [6], [8], [13], [14], [15] or to a shared common space [16], [17], [18], [19], to extract the relationship between visual features and semantic features. However, semantic-visual embedding always faces the challenge of semantic insufficiency, which will lead to incomplete expression of semantic and visual features in embedding. Especially for two similar categories, it is difficult to learn discriminative features. To solve this problem, many effective methods have been proposed to improve the expression of semantic and visual features, including attention-based methods [20], [21], [15], [22] and knowledge graph-based methods [23], [24], [25]. Attention-based methods enhance the expression of visual and semantic features by making the model focus on more fine-grained visual or semantic features; Knowledge graph-

based methods enrich the expression of semantic and visual features by aggregating node information around categories. However, the semantic diversity of these two methods is limited by the dataset itself and does not generate any new semantic information. We summarized several phenomena that need to be improved in semantic-to-visual embedding: 1) The model needs to map more discriminative semantic features to visual features. As shown in Fig.1(b), "White nick" is an important attribute that distinguishes "White necked Raven" from "Brewer Blackbird". The proposed method enhances the learning of this attribute by increasing the importance of this attribute and reducing the importance of others; 2) The model needs to have a stronger ability to find insignificant semantic-to-visual embedding. As shown in Fig.1(c), the "White tip" attribute is difficult to correspond visually because it is not obvious visually. The proposed method implicitly reduces the importance of other attributes to force the model to learn its semantic-to-visual mapping relationship.

2) *The Domain-Shift Challenge*: The domain-shift challenge in ZSL was first identified by [26], which is caused by the huge difference between the seen and unseen classes in the semantic space and visual space. For example, the "tails" of pigs and zebras are not semantically different, but they are very different visually. To solve this problem, many transductive ZSL approaches [27], [28], [29], [30] have been proposed. They integrate the data of seen and unseen categories to learn more general visual-semantic embeddings. However, this method is unreasonable because it is difficult for us to get the relevant data of unseen classes from the beginning in the real scene. Therefore, in most cases, these methods do not have strong generalization. Similarly, we also summarized several unresolved phenomena in the domain-shift: 1) The seen classes have the visual features of the unseen classes, but it lacks the semantic information of the unseen classes in semantic-to-visual embedding. As shown in Fig.1(d), the attribute "black throated" does not exist in the seen class "White necked Raven" but exists in the unseen class "black-throated sparrow", they all have the same visual features. Our method alleviates this phenomenon by generating new and reliable semantic features; 2) The unrestricted search space of the model leads to more prone to domain-drift. As shown in Fig.1(e), our approach limits the visual space by generating offset visual features, so that the synthesized visual features can deviate to the unseen category.

In this paper, in order to alleviate these two challenges, we propose a new generative zero-shot learning method. The proposed method uses the two modules, including Multi-Knowledge Fusion Network (MKFNet) and New Feature Generator (NFG), to deal with the semantic insufficiency challenge and domain-shift challenge. Following our previous work [31], the proposed method first builds a three-level knowledge hierarchy according to the taxonomic Family-Genus-Species knowledge. Note that the level from low to high is Species, Genus, Family. Compared with the low-level knowledge, the high-level knowledge have higher universality or generalization and lower specificity for model learning, as shown in Fig.1(a). Then the MKFNet is trained by using different semantic features from multi-knowledge domain to obtain more

semantic information, and the proposed knowledge regularization term L_{KR} is used to generate visual features belonging to different knowledge, which will imply unseen information. Finally, more generalized visual features are generated by adaptively fusing different synthesized visual features from multi-knowledge. Meanwhile, the proposed NFG adds new semantic features including enhanced and novel ones. The enhanced regularization term L_{ER} and novel regularization term L_{NR} are used to further enrich semantic knowledge and generate visual features that deviate to unseen samples. In summary, the main contributions of this paper are as follows:

- We propose a new generative ZSL model, Multi-Knowledge Fusion Network (MKFNet), to adaptively fuse different visual features from multi-knowledge domain for synthesizing more generalized visual features.
- We propose the New Feature Generator (NFG) to generate new semantic features for each knowledge domain, including enhanced semantic features and novel semantic features, to make the MKFNet learn more semantic information and generate visual features that intersect with unseen classes.
- Extensive experiments on seven major benchmarks show that the proposed approach achieves state-of-the-art performances on both the traditional ZSL and the generalized ZSL tasks.

II. RELATED WORKS

A. Generative ZSL

Recently, generative methods dominate ZSL, which reduces ZSL to a traditional classification problem. [32], [6], [33], [34], [35] used the existing generative model or its variants to synthesize visual features by using category semantics and random noise. The difference is that [32] proposed a one-to-one mapping approach where synthesized visual features are restricted; [6] introduced visual center regularization to make the synthesized visual features close to the center of the class; [33] improved the performance of the generator by adding auxiliary classifier; [34] used the encoder-decoder structure to constrain the generation of visual features, so as to get a better generator; [35] projected the original visual features into a new (redundancy-free) space to learn the redundancy-free features. Our model is also a generative method, which generates more generalized visual features by using semantic features from multi-knowledge as input. In the previous generative methods, several are closely related to our model. For example, GDAN [36] used semantic-to-visual and visual-to-semantic multiple mapping to retrain enough semantic information; DGP [23] and APNet [25] obtained more semantic features by constructing a knowledge graph and aggregating the information of neighbor nodes. Although this method can alleviate the problem of semantic insufficiency and domain shift to a certain extent, it does not directly produce informations of unseen classes. In contrast, our method compensates for the lack of semantics by adding semantic information of different knowledge and adaptively generating more semantic features. In addition, the proposed approach uses L_{KR} regularization to enable our synthesized samples to deviate to unseen classes.

B. Attention-based approach

The purpose of the attention mechanism is to highlight important local information, or to shield the influence of irrelevant information or noise information. Due to its effectiveness and versatility, the attention mechanism has been widely used in various computer vision tasks, such as image classification[37], [38], image segmentation[39], [40], image generation[41], [42], etc. Recently, a large number of attention-based methods [20], [21], [15], [22] have been proposed for ZSL recognition tasks. For instances, [20] proposed a stacked semantics-guided attention (S²GA) model to obtain semantic related features by using individual category semantic features to progressively guide visual features to generate attention maps for weighting the importance of different local regions; [15] proposed a dense attribute-based attention mechanism, which focuses on the most relevant image regions for each attribute and obtains attribute-based features. Although these attention-based methods improved the performance of the model by mining local semantic or visual features, they easily lead to overfitting in semantic-visual embedding. In this paper, we propose a Multi-Knowledge Fusion Network (MKFNet) with adaptive fusion module based on the attention mechanism, which combines the visual features of different knowledge and tries to find the optimal visual weight between different knowledge to generate more generalized samples.

C. Genetic-based Approach

Genetic algorithm is a randomized and optimized method guided by the principles of evolution and natural genetics. It is widely used in various tasks [43], [44], [45], [46] because of its high efficiency, adaptability and robustness. And it can produce near-optimal solutions and can handle large, highly complex and multi-modal spaces. For instances, [43] proposed an automatic CNN architecture design method by using genetic algorithms, to effectively address the image classification tasks. [44] used genetic evolutionary operations, including selection, mutation and crossover to evolve a population of DCNN architectures. To our best knowledge, there is no work to utilize the genetic algorithm to ZSL task. In our work, we proposed a New Feature Generator (NFG) with adaptive genetic algorithm for ZSL, which uses mutation and crossover strategies to generate new semantic features and uses a similarity-based selection strategy to adaptively filter new semantic features into enhanced and novel semantic features. Specially, NFG uses two regularization terms L_{ER} and L_{NR} to further alleviate the problems of semantic insufficiency and domain-shift, respectively.

III. THE PROPOSED APPROACH

In this section, we first introduce the overall architecture of the proposed approach in Section III-A. Then the Multi-Knowledge Fusion Network (MKFNet) and the implementation of the adaptive fusion module are explained in Section III-B and Section III-C, respectively. After that, New Feature Generator (NFG) is described in detail in Section III-D. Finally, we discuss the training and testing process of the proposed approach in Section III-E .

A. The Model Architecture

The Fig.2 shows the model architecture of the proposed method. It is obviously that the proposed approach is based on generative model and our Multi-Knowledge Fusion Network (MKFNet) consists of three generators belonging to different knowledge and one discriminator. The generator of the GAZSL [6] is selected as skeletons of generators G_{Family} , G_{Genus} and $G_{Species}$, and the discriminator of GAZSL is selected as skeleton of the discriminator of the proposed MKFNet. The detailed process of the proposed method is described as the following steps:

Feature Extraction: For any dataset, we need to extract visual features from images and semantic features from attributes or text, respectively. For details, see Semantic Representation and Visual Representation in IV-A.

Multi-Knowledge Fusion Network (MKFNet): Following our previous work [31], the hierarchy of the three knowledge (Species, Genus, Family) is first constructed according to class names and biological taxonomy. Then, three semantic features of different knowledge are input into the corresponding generators to synthesize visual features $\tilde{x}_i^{Species}$, \tilde{x}_i^{Genus} and \tilde{x}_i^{Family} , and the adaptive fusion module will weight these synthesized visual features to obtain the final visual features \tilde{x}_i , as shown in the Fig.3. The real visual features of the corresponding species and the final visual features are input into the discriminator for real and fake discrimination and label classification.

New Feature Generator (NFG): NFG uses the original semantic features from different knowledge as the input of the adaptive genetic strategy (see Fig.4 for details) to generate more new semantic features, including enhanced semantic features and novel semantic features. Enhanced semantic features are used to supplement more semantic information for each original knowledge domain, and new semantic features are used for unsupervised training of MKFNet to improve the generalization ability of the model.

B. Multi-Knowledge Fusion Network

In order to solve the zero-shot classification task, a model needs to be trained to infer the unseen categories from the corresponding class semantic prototypes. To achieve this goal, we design a Multi-Knowledge Fusion Network (MKFNet) to map semantic features into visual space. In short, MKFNet is a generative adversarial network, which consists of three generators and a discriminator.

Previous zero-shot learning methods usually use a single semantic feature to learn semantic-to-visual embedding, which obviously leads to insufficient semantics. We follow our previous work [31] to use a variety of relevant semantic features to learn, which obviously increase more semantic information. Following [31], we can construct a Family-Genus-Species hierarchy of three knowledge for original dataset according to taxonomy. The hierarchical relationship between different knowledge is Family > Genus > Species. Higher level knowledge include lower level knowledge, such as Genus are subsets of Family and Species are subsets of Genus. The

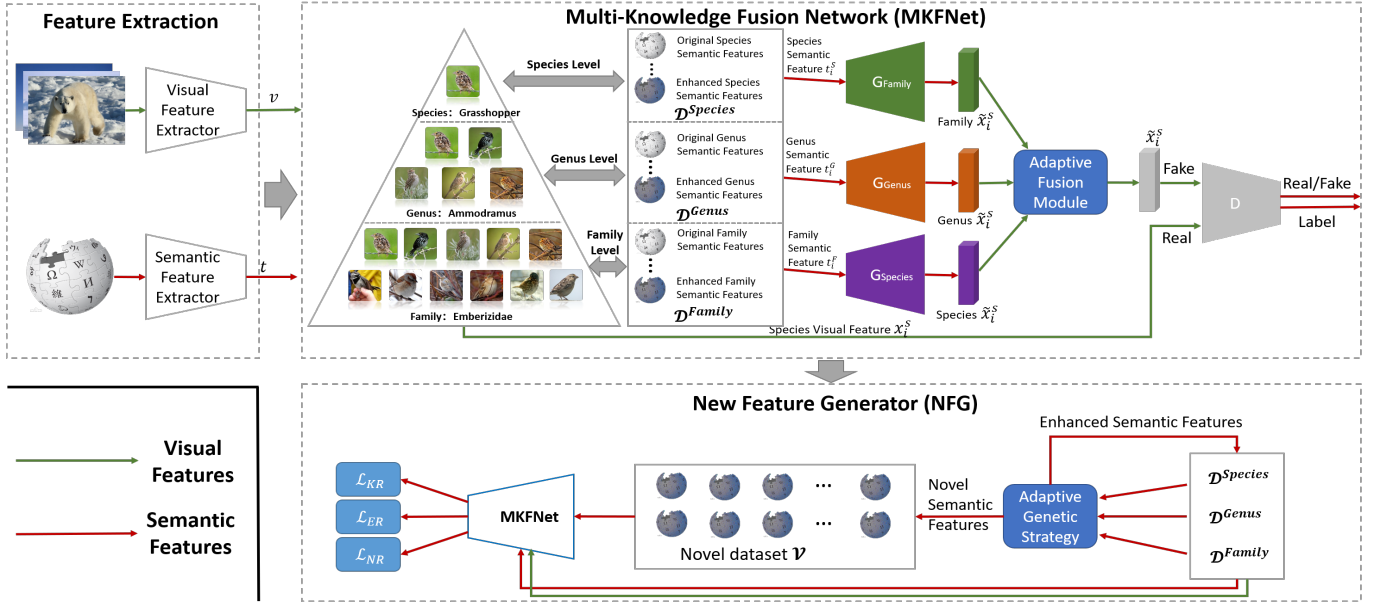


Fig. 2. The overall framework of the proposed approach.

final structure is shown in Fig.1(a). We formalize the datasets \mathcal{D}^{Family} , \mathcal{D}^{Genus} , and $\mathcal{D}^{Species}$ of different knowledge as:

$$\mathcal{D}^\bullet = (x_i^s, y_i^s, t_i^{s,\bullet}), i = 1, \dots, N^s \quad (1)$$

Where N^s is the total number of seen class samples, \bullet can be represented Species, Genus and Family. $t_i^{s,Species}$, $t_i^{s,Genus}$ and $t_i^{s,Family}$ denote semantic features belonging to the same Species, Genus and Family, respectively. Note that the y_i^s in Genus and Family will be replaced with the new class labels of corresponding Genus and Family. Obviously, visual feature x_i^s in the same Family will include visual features of multiple Genus or Species.

MKFNet uses three generators to learn information about three different knowledge, which are $G_{Species}$, G_{Genus} and G_{Family} . The generator of each knowledge is used to map semantic features to visual space $\mathbb{R}^S \rightarrow \mathbb{R}^V$. Obviously, generator with higher knowledge will learn more generalized visual features. In order to make each model learn the semantic-to-visual mapping of different knowledge better, the knowledge regularization term is added to these generators to make the synthesized visual features close to the visual center of the corresponding knowledge. The knowledge regularization terms of generators $G_{Species}$, G_{Genus} and G_{Family} are formalized as follows:

$$L_{KR}^{Species} = \frac{1}{N^s} \sum_i \|G_{Species}(t_i^s, z) - \hat{x}_i^{s,Species}\|^2 \quad (2)$$

$$L_{KR}^{Genus} = \frac{1}{N^s} \sum_i \|G_{Genus}(t_i^s, z) - \hat{x}_i^{s,Genus}\|^2 \quad (3)$$

$$L_{KR}^{Family} = \frac{1}{N^s} \sum_i \|G_{Family}(t_i^s, z) - \hat{x}_i^{s,Family}\|^2 \quad (4)$$

Where N^s is the total number of seen samples, and $G_\bullet(t_i, z)$ is the visual feature generated by G_\bullet according to semantic feature t_i and random noise z . $\hat{x}_i^{s,Species}$ represents the visual feature center of all categories belonging to y_i^s 's Species. Similarly, $\hat{x}_i^{s,Genus}$ and $\hat{x}_i^{s,Family}$ denote the visual center of Genus and Family corresponding to y_i^s , respectively. L_{KR} regularization force the synthesized visual features to deviate to the unseen class by closing to the class center of higher level knowledge, which increases the generalization ability of the generator. The loss of these generators are defined as:

$$L_G^\bullet = -\mathbb{E}[D(G_\bullet(\mathcal{T}, z))] + L_{cls}(G_\bullet(\mathcal{T}, z)) + L_{KR}^\bullet \quad (5)$$

Where the first term is Wasserstein loss [47], and the second term is cross-entropy loss of classification. \bullet can be represented as Species, Genus, or Family. For example, $L_G^{Species}$ represents the loss of $G_{Species}$.

After generating three visual features $\tilde{x}_i^{s,Species}$, $\tilde{x}_i^{s,Genus}$ and $\tilde{x}_i^{s,Family}$ belonging to different knowledge by using $G_{Species}$, G_{Genus} and G_{Family} , the final synthesized visual feature \hat{x}_i^s is obtained through an attention-based adaptive fusion module, which fuses visual information of different knowledge. See section III-C for details. D is the discriminator, which has the same structure as the discriminator of ACGAN [48]. The discriminator D first receives the final synthesized visual features \hat{x}_i^s and real visual features corresponding to Species as input. Then these two visual features are forwarded through two full connected layers. Subsequently, there are two output branches: the first branch is used for binary classifier to distinguish whether the input features are real or fake; the second one classifies the input samples into correct classes. The loss function of the discriminator D is the same with the previous work [6].

C. Adaptive Fusion Module

To solve the problem of feature fusion from different knowledge, features summing is a simple and common approach, which can perform the summing operation on the output $\tilde{x}_i^{s,Species}$, $\tilde{x}_i^{s,Genus}$ and $\tilde{x}_i^{s,Family}$ from $G_{Species}$, G_{Genus} , and G_{Family} to obtain the fusion feature \tilde{x}_i^s . We can easily perform this operation because the output of each generator has the same dimensions as the visual features. The operation is formalized as:

$$\tilde{x}_i^s = \frac{\tilde{x}_i^{s,Family} + \tilde{x}_i^{s,Genus} + \tilde{x}_i^{s,Species}}{3} \quad (6)$$

However, the features summing method is unreasonable that the above-mentioned fusion method treat three visual features from different knowledge with equal importance. In practice, due to the inconsistent distribution of different knowledge domains, these visual features from different knowledge has different contributions to the final synthesized visual features. For example, the universality of Family, Genus, and Species sequentially decreases, and the specificity increases sequentially. Therefore, it is very necessary to assign weights reasonably to visual features of different knowledge. To handle these situation, we propose an adaptive fusion module to automatically assign importance weights to these three visual features. Inspired by attention mechanism [37], [38], we apply the same ideas into our method to learn the importance weights. Fig.9 visually shows the overall architecture of the adaptive fusion module. The input features $\tilde{x}_i^{s,Species}$, $\tilde{x}_i^{s,Genus}$ and $\tilde{x}_i^{s,Family}$ are projected by a full connected layer with LeakyReLU into three vectors of the same dimensionality. Let W_1^\bullet and b_1^\bullet denote the projection (weight) matrix and the bias vector of the first full connected layer that directly takes the visual features of Family, Genus and Species as the input. \bullet can be represented as Family, Genus and Species. Subsequently, the three projected visual features are passed through a nonlinear activation function σ_1 , which is chosen to be the LeakyReLU function in this paper. The output of the first layer is formalized as $\sigma_1(W_1^\bullet \tilde{x}_i^{s,\bullet} + b_1^\bullet)$.

Furthermore, the output of the first layer is propagated forward to a full connected layer, which has only one output neuron. We define the weight matrix and bias vector of the second layer as W_2^\bullet and b_2^\bullet , and the activation function as σ_2 (which is Sigmoid in this paper). As a result, the importance weight is predicted as a scalar score, which is formalized as:

$$s^\bullet = \sigma_2(W_2^\bullet(\sigma_1(W_1^\bullet \tilde{x}_i^{s,\bullet} + b_1^\bullet)) + b_2^\bullet) \quad (7)$$

In order to ensure the consistency of the visual features before and after the fusion, the normalization layer is used to normalize the three scalars. The normalized scalar is used as the final importance weight, denoted by ρ^{Family} , ρ^{Genus} , and $\rho^{Species}$ respectively. They are formalized as:

$$\rho^\bullet = \frac{s^\bullet}{s^{Family} + s^{Genus} + s^{Species}} \quad (8)$$

Finally, we can obtain the fusion feature \tilde{x}_i^s by a weighted sum, which is formulated as:

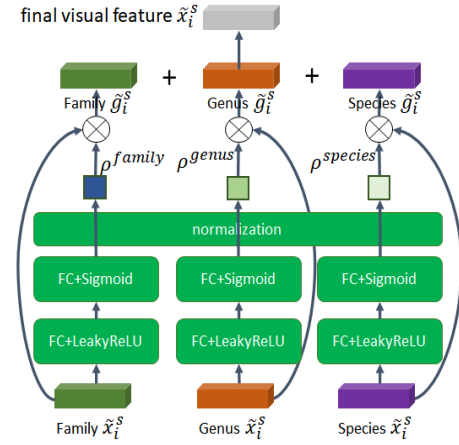


Fig. 3. The detail of the adaptive fusion module.

$$\tilde{x}_i^s = \rho^{Family} \tilde{x}_i^{s,Family} + \rho^{Genus} \tilde{x}_i^{s,Genus} + \rho^{Species} \tilde{x}_i^{s,Species} \quad (9)$$

The loss function of the adaptive fusion module is formalized as:

$$L_{FM} = -\mathbb{E}[D(\tilde{x}^s)] - \mathbb{E}[\sum_{k=1}^{K^s} y_k \log(D(\tilde{x}^s))] + L_{ER} + L_{NR} \quad (10)$$

Where, the first term tricks the discriminator to classify synthesized visual features from generator as real and the second term is classified cross-entropy loss. The third and fourth terms will describe in Section III-D. \tilde{x}^s is obtained according to the Formula 9.

D. New Feature Generator

The whole process of New Feature Generator (NFG) is shown in Fig.4. In order to obtain the new semantic features \tilde{t}^s from different knowledge, we first randomly sample two semantic features $t_a^s, t_b^s \in \mathcal{T}$ from any category of $\mathcal{D}^{Species}$, \mathcal{D}^{Genus} and \mathcal{D}^{Family} . Note that every dataset \mathcal{D}^\bullet should be considered. In particular, the Fig.4 shows the new semantic generation process with the Genus label Ammodramus, so two semantic features need to be randomly sampled from all the semantic features with the Genus label Ammodramus. Then, the semantic feature \tilde{t}^s is obtained through two operations: the mutation of a single semantic feature t_a^s or t_b^s and the crossover between a pair of semantic features t_a^s and t_b^s . See detail in Algorithm 1. Finally, the semantic features \tilde{t}^s derived from mutation and crossover are input into the proposed MKFNet to synthesize visual features \tilde{x}^s and the cosine similarity d is calculated using real visual features x^s and synthesized visual features. The calculation process is formalized as:

$$d = \frac{\tilde{x}^s \cdot x^s}{|\tilde{x}^s| |x^s|} \quad (11)$$

Where \cdot represents the dot product of vectors and $|x^s|$ represents the modulus of the vector x^s . The semantic features \tilde{t}^s whose similarity are higher than the stability coefficient

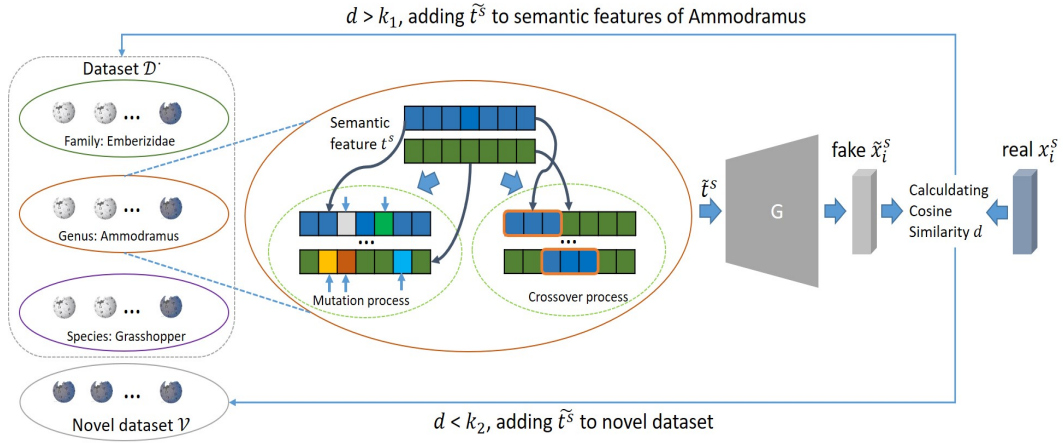


Fig. 4. The whole process of the adaptive genetic strategy. Take Genus Ammodramus as an example. First, randomly sample two semantic features t_a^s and t_b^s from the semantic features of Ammodramus, and use them to generate new semantic features \tilde{t}^s through the mutation process and the crossover process, see Algorithm 1 for details. Then, the cosine similarity d is calculated by using the synthesized visual feature, which is generated by inputting the new semantic feature \tilde{t}^s into MKFNet, and the real visual feature. Finally, if the d is greater than the stability coefficient κ_1 , it is regarded as enhanced semantic features and added to the semantic features of Ammodramus. If the d is less than the stability coefficient κ_2 , it is regarded as novel semantic features and added to the novel dataset. κ_1 and κ_2 satisfy $\kappa_1 > \kappa_2$.

κ_1 ($d > \kappa_1$) will be viewed as enhanced semantic features $\tilde{t}_{enhanced}^s$ and added to the dataset to which semantic features t_a^s and t_b^s belong. The dataset \mathcal{D}^\bullet will be updated as:

$$\mathcal{D}^\bullet = (x_i^s, y_i^s, \{t_i^s \cup \tilde{t}_{enhanced}^s\}), i = 1, \dots, N^s \quad (12)$$

Where $\tilde{t}_{enhanced}^s$ represents the high-stability semantic features generated by NFG. The semantic feature \tilde{t}^s whose similarity is lower than the stability coefficient κ_2 ($d < \kappa_2$) will be viewed as novel semantic features \tilde{t}_{novel}^s and added to the novel dataset \mathcal{V} . The novel dataset is defined as:

$$\mathcal{V} = \{\mathcal{V} \cup \tilde{t}_{novel}^s\} \quad (13)$$

Where \tilde{t}_{novel}^s represents all low-stability semantic features generated by NFG and the low-confidence semantic feature is considered to have deviated to the unseen category. For $\tilde{t}_{enhanced}^s$ added to the corresponding datasets ($\mathcal{D}^{Species}$, \mathcal{D}^{Genus} or \mathcal{D}^{Family}), they are continuously trained as the semantic features of the corresponding class label, and their loss function is formalized as:

$$L_{ER} = -\mathbb{E}[D(G(\tilde{t}_{enhanced}^s, z))] - \mathbb{E}[\sum_{n=1}^{N^s} y_k \log(D(G(\tilde{t}_{enhanced}^s, z)))] \quad (14)$$

Where, N^s represents the total number of seen classes. For \tilde{t}_{novel}^s in the novel dataset, they have no visual features and category labels. We use unsupervised novel regularization L_{NR} to optimize the generative model, so that the generator can learn more unseen information. Its regularization term L_{NR} is defined as:

$$L_{NR} = \mathbb{E}[D(G(\tilde{t}_{novel}^s, z))] + \lambda L_2[D(G(\tilde{t}_{novel}^s, z)), \tilde{y}] \quad (15)$$

Where the first term tricks the discriminator to classify synthesized visual features from generator as fake and the second term is L_2 regularization to calculate the distance from the class distribution to the uniform distribution \tilde{y} . The \tilde{y} is defined

as a vector whose dimension is the number of seen classes K^s and all values are $\frac{1}{K^s}$. λ is penalty coefficient.

Algorithm 1: The processes of mutation and crossover.

Input: t_a^s, t_b^s , the dimension of semantic feature d

Output: semantic features v_{mut} and v_{cross}

- 1 Random sampling a mutation coefficient r_1 and a crossover coefficient r_2 from uniform distribution $U(0, 1)$.
 - 2 Random selecting $d * r_1$ and $d * r_2$ locations loc_1 and loc_2 for mutation and crossover, respectively.
 - 3 Let the semantic feature of mutation and crossover be $v_{mut} = t_a^s$ and $v_{cross} = t_b^s$ respectively.
 - 4 **for** $i = 1; i \leq d * r_1; i++$ **do**
 - 5 Sampling a random number r from $U(0, 1)$
 - 6 **if** $v_{mut}[loc_1[i]] \neq 0$: $v_{mut}[loc_1[i]] * r$
 - 7 **else**: $v_{mut}[loc_1[i]] + r$
 - 8 **end**
 - 9 **for** $i = 1; i \leq d * r_2; i++$ **do**
 - 10 $v_{cross}[loc_2[i]] = t_b^s[loc_2[i]]$
 - 11 **end**
-

E. Learning Scheme

After we obtain the three datasets of different knowledge $\mathcal{D}^{s,Species}$, $\mathcal{D}^{s,Genus}$ and $\mathcal{D}^{s,Family}$, we select three sample points $(x^{s,\bullet}, y^{s,\bullet}, t^{s,\bullet})$ from them and input their semantic features into corresponding generator to obtain the synthesized visual features $\tilde{x}^{Species}$, \tilde{x}^{Genus} and \tilde{x}^{Family} . Note that the three selected sample points must belong to the same Family. Then, the knowledge regularization L_{KR}^\bullet of each generator is calculated according to the synthesized visual features. Next, these synthesized visual features are all propagated forward to the fusion model to get the final visual features \tilde{x}^s . Finally, the synthesized visual features \tilde{x}^s are input into the discriminator

and the loss function L_{FM} of the fusion model, the loss function L_D of the discriminator, and the loss function L_G^\bullet of the generator are calculated. After iterative training of the above steps N_{NFG} times, NFG with two regularization terms L_{ER} and L_{NR} is used to enrich semantic information and learn the information deviated to unseen classes. The training procedure of the proposed MKFNet is showed in Algorithm 2.

In testing, the visual features in unseen classes can be synthesized by three generators conditioned on a given unseen semantic feature t^u , as $\tilde{x}^{u,Family} = G_{Family}(t^u, z)$, $\tilde{x}^{u,Genus} = G_{Genus}(t^u, z)$ and $\tilde{x}^{u,Species} = G_{Species}(t^u, z)$. And the final visual features \tilde{x} can be obtained by adaptive fusion module. By this way, we can generate a large of synthesized visual features by sampling different z for the sample text t^u . Finally, the class label of unseen visual feature x^u can be determined by finding the label corresponding to the synthesized visual feature that is the most similar to the real visual feature.

IV. EXPERIMENTS

A. Experimental Settings

Datasets: We use seven common datasets to evaluate the proposed approach, which are three text-based recognition datasets and four attribute-based recognition datasets, respectively. The former include Caltech-UCSD-Birds 200-2011 (CUB) [49], North America Birds (NAB) [50] and Oxford 102 Flowers (FLO) [51]; The latter use GBU-setting [7] and include CUB-Att [49], Animals with Attributes 1 (AwA1) [52], Animals with Attributes 2 (AwA2) [53], attributes Pascal and Yahoo (aPY) [54]. For CUB and NAB datasets, two schemes [5] are proposed to split the classes into training/testing (in total four benchmarks): Super-Category-Shared (SCS) or easy split and Super Category-Exclusive Splitting (SCE) or hard split. These two splits represent the similarity between the seen and unseen classes, so the former represents a higher similarity than the latter. For CUB-Att, AwA1, AwA2 and aPY datasets, the standard zero-shot splits provided by [53] is adopted. For FLO dataset, the splits provided by [51] is used. The statistical information about these datasets is given in Table.I.

Semantic Representation: We use the raw Wikipedia articles extended by [5] for both CUB and NAB. Like the textual representation method of [6], [8], we use the same preprocessing method and use Term Frequency-Inverse Document Frequency (TF-IDF) vectors as the semantic representation of Wikipedia articles. For FLO, we use the fine-grained visual descriptions collected by [55]. The 1024-dim character-based CNN-RNN [55] features are extracted from fine-grained visual descriptions (10 sentences per image). None of the \mathcal{Y}^u sentences are seen during training the CNN-RNN. We build per-class sentences by averaging the CNN-RNN features that belong to the same class. Refer to [33], [56] for more details. For CUB-Att, AwA1, AwA2, and aPY datasets, we directly obtain the category attributes provided in the original dataset as semantic labels.

Visual Representation: For CUB and NAB, fine-grained visual features are extracted by using the part-based FC layer in VPDE-net [57]. See [6], [8], [33], [53] for details. There

Algorithm 2: The training procedure of the proposed MKFNet.

Input: the maximal loops $Step$, the start loop of NFG N_{NFG} , the stability coefficient κ_1, κ_2 .

- 1 Obtain $D^{s,Species}$, $D^{s,Genus}$ and $D^{s,Family}$ using Eq. 1.
- 2 Initialize the novel dataset $\mathcal{V} = \emptyset$.
- 3 Calculate visual centers $\hat{x}^{Species}$, \hat{x}^{Genus} , \hat{x}^{Family} for each class in $D^{s,Species}$, $D^{s,Genus}$ and $D^{s,Family}$, respectively.
- 4 **for** $i = 1; i \leq Step; i++$ **do**
- 5 **if** $i > N_{NFG}$ **then**
- 6 obtain new semantic features \tilde{t} using Algorithm 1
- 7 Get the visual features \tilde{x} with \tilde{t} by using Eq. 9.
- 8 Calculate the cosine similarity d between \tilde{x} and x .
- 9 **if** $d > \kappa_1$ **then**
- 10 Add \tilde{t} to $\mathcal{D}^{s,Species}$, $\mathcal{D}^{s,Genus}$, or $\mathcal{D}^{s,Family}$.
- 11 **end**
- 12 **if** $d < \kappa_2$ **then**
- 13 Add \tilde{t} to \mathcal{V} .
- 14 **end**
- 15 **end**
- 16 **for** $j = 1; j \leq 5; j++$ **do**
- 17 Sample a minibatch of images x , matching texts $t^{s,\bullet}$, random noise z .
- 18 $\tilde{x}^\bullet \leftarrow G_\bullet(t^{s,\bullet}, z)$.
- 19 Get the final visual features \tilde{x} by using Eq. 9.
- 20 Calculate the discriminator loss L_D by x and \tilde{x} .
- 21 Update discriminator parameters using Adam.
- 22 **end**
- 23 Sample a mini-batch of class labels y , matching texts $t^{s,\bullet}$, random noise z .
- 24 Get the final visual features \tilde{x} by using Eq.9.
- 25 Calculate L_{KR}^\bullet by Eq. 2, 3, 4 and L_G^\bullet by Eq. 5.
- 26 Calculate L_{ER} by using Eq. 14.
- 27 Sample texts \tilde{t}_{novel} from \mathcal{V} .
- 28 Generate final visual features \tilde{x} using \tilde{t}_{novel} and calculate L_{NR} according to Eq. 15.
- 29 Calculate loss function L_{FM} by using Eq. 10.
- 30 Update parameters of generators using Adam(∇L_G^\bullet).
- 31 Update parameters of adaptive fusion module using Adam(∇L_{FM})
- 32 **end**

are seven image-parts be detected in CUB dataset, which are head, back, belly, breast, leg, wing and tail. In NAB dataset, the "leg" part is missing because there is no annotation for this part in the original dataset. At last, the full dimensions of visual features in CUB and NAB are 3584D ($512D \times 7$ parts) and 3072D ($512D \times 6$ parts) respectively. Following [6], [8], [33], [53], we use the top pooling units of the ResNet-101 [1] pre-trained on ImageNet-1K as the visual features for the rest

TABLE I

THE STATISTICAL INFORMATION OF NINE BENCHMARKS. $|\mathcal{T}|$ REPRESENT THE DIMENSION OF SEMANTIC FEATURE. ATT? EQUALS Y TO REPRESENT SEMANTIC FEATURE BASED ON ATTRIBUTE, OTHERWISE N FOR SEMANTIC FEATURE BASED ON WIKIPEDIA TEXT. $|\mathcal{X}|$ REPRESENT THE NUMBER OF IMAGES. $|\mathcal{Y}|$ REPRESENT THE NUMBER OF ALL CLASSES, $|\mathcal{Y}^s|$ REPRESENT THE NUMBER OF CLASSES IN TRAINING+VALIDATION, AND $|\mathcal{Y}^u|$ REPRESENT THE NUMBER OF TEST CLASSES.

Dataset	$ \mathcal{T} $	att?	$ \mathcal{X} $	$ \mathcal{Y} $	$ \mathcal{Y}^s $	$ \mathcal{Y}^u $
CUB(SCS)	7551	N	11788	200	120+30	50
CUB(SCE)	7551	N	11788	200	130+30	40
NAB(SCS)	13217	N	48562	404	200+123	81
NAB(SCE)	13217	N	48562	404	200+123	81
FLO	1024	N	8189	102	62+20	20
CUB-Att	312	Y	11788	200	100+50	50
AwA1	85	Y	30475	50	27+13	10
AwA2	85	Y	37322	50	27+13	10
aPY	64	Y	15339	32	15+5	12

of datasets. Thus, those visual features can be represented as a 2048D vectors. For FLO, CUB-Att, AwA1, AwA2 and aPY, the 2,048-dimensional visual features are directly extracted by ResNet-101 [1] pretrained on ImageNet.

Evaluation Metrics: We use three metrics [4], [6], [8], [12], [35] widely used in evaluating ZSL recognition performance: Top-1 unseen class accuracy, Area under Seen-Unseen curve (AUSUC) and harmonic mean (H). The first one is standard ZSL evaluation, which evaluates the performance on single domain (unseen domain). And the last two are generalized ZSL evaluation, which evaluates the performance on two domains (seen and unseen domains). The harmonic mean is denoted by $H = (2S \times U)/(S + U)$. S and U are the Top-1 Accuracies for seen and unseen domains.

Implementation Details: We implement our model with neural networks using PyTorch. For each generator (G_{Family} , G_{Genus} and $G_{Species}$) and discriminator D in MKFNet, the skeleton and parameter settings are consistent with GAZSL [6] which will be used as the baseline of our model for comparison. We use Adam solver with $\beta_1 = 0.5$ and $\beta_2 = 0.9$. We empirically set the total number of iterations $N_{NFG} = 3$, the stability coefficient $\kappa_1 = 0.8$, $\kappa_2 = 0.2$. The full source code of our model can be found at github¹.

B. Comparison with state-of-the-art methods

Experimental Results on CUB and NAB: The CUB and NAB datasets are used to evaluate the performance of the proposed method on Wikipedia articles. Table II shows the state-of-the-art results on CUB and NAB with easy and hard splittings. We observe that the proposed method achieves significant improvements over the Baseline18 and the state-of-the-art methods in terms of both Top-1 accuracy and Seen-Unseen AUC. Specially, in the hard splitting of CUB and NAB, the proposed method achieves 54.4% and 40.7% improvements on Top-1 accuracy metric, 65.5% and 46.6% improvements on Seen-Unseen AUC metric, compared with Baseline18. In the easy splitting of CUB and NAB, the proposed method achieves 8.7% and 3.1% improvements on

Top-1 accuracy metric, 14.4% and 13.7% improvements on Seen-Unseen AUC metric, compared with Baseline18. Compared with the state-of-the-art methods, the proposed method achieves 3.7% and 10.4% improvements on Top-1 accuracy metric, 0.7% and 15.2% improvements on Seen-Unseen AUC metric respectively in easy and hard splittings of CUB. In easy and hard splittings of CUB, the proposed method achieves an improvement of up to 30.1% under Top-1 and AUC metrics.

Experimental Results on CUB-Att, AwA1, AwA2, FLO and aPY: In these five benchmarks, we used new metrics (U , S and H) to evaluate the performance of our approach. In order to evaluate that our approach is still effective under different semantic representations, CUB-Att, AwA1, AwA2 and aPY with GBU-setting is applied to change the semantic representation from Wikipedia articles to attributes. The evaluation results of S , U and H on CUB-Att, AwA1, AwA2, FLO and aPY are given in Table III. We observe that the proposed approach surpassed state-of-the-art methods on most evaluation metrics in these five datasets. Specially in H metric, the H value improvement on AwA1 increases from 72.1% to 76.4%, on AwA2 increases from 67.1% to 74.0%, on FLO from 76.0% to 83.7%. Compared with the generative ZSL methods [6], [33], [65], [36], [66], the performance of our method has been consistently improved on almost all evaluation metrics, and the highest improvement is 23.4% in the U metric of the FLO dataset. Remarkably, compared with Baseline18, the proposed method achieves a very significant improvement, e.g., 172.6% and 112.7% improvements of U metric on FLO and aPY. This demonstrates the effectiveness of the proposed method in generating more discriminative visual features.

C. Ablation Studies

In this section, we performed ablation experiments on several important components of the proposed method. To evaluate the impact of the adaptive fusion module, we use simple features summing operation instead of the adaptive fusion module, denoted as MKFNet-base. To evaluate the effectiveness of the MKFNet, we use CKL-TR [31] (which is our previous work) as the baseline because our method is improved based on it and uses the new proposed generative model. The terms MKFNet and MKFNet-NFG indicate using NFG method and not using NFG method respectively and they all uses the adaptive fusion module. The results are reported in Table.IV. Compared with MKFNet-base, our MKFNet has achieved a consistent improvement in all metric, which represents that the adaptive fusion module can produce more appropriate weights effectively and automatically to fuse better visual features. we can see that MKFNet-base has a higher accuracy in the seen classes, 67.1% than 63.3%, indicating that the visual features generated by the simple features summing has poor generalization because it has a little over-fitting in the seen class. Compared with CKL-TR, our MKFNet has achieved a consistent improvement in H metric, which shows that the proposed generative model can synthesize more generalized visual features. Especially in CUB-Att, the H metric is improved from 53.7% to 60.0%. A reasonable reason is that the fine-grained CUB dataset is more densely distributed in the visual

¹<https://github.com/a494456818/MKFNet-NFG>

TABLE II

RESULT OF ZSL IMAGE CLASSIFICATION ON **CUB** AND **NAB**. WE REPRODUCE THE RESULTS OF GDAN, WHOSE SOURCE CODE IS AVAILABLE ONLINE. THE RED VALUE REPRESENT THE INCREASING NUMBER COMPARED WITH THE BASELINE18.

methods	Top-1 Accuracy				Seen-Unseen AUC			
	CUB		NAB		CUB		NAB	
	Easy	Hard	Easy	Hard	Easy	Hard	Easy	Hard
WAC-Linear[58]	27.0	5.5	-	-	23.9	4.9	23.5	-
WAC-Kernel[59]	33.5	7.7	11.4	6.0	14.7	4.4	9.3	2.3
ESZSL[60]	28.5	7.4	24.3	6.3	18.5	4.5	9.2	2.9
ZSLNS[61]	29.1	7.3	24.5	6.8	14.7	4.4	9.3	2.3
SynC _{fast} [62]	28.0	8.6	18.4	3.8	13.1	4.0	2.7	3.5
ZSLPP[63]	37.2	9.7	30.3	8.1	30.4	6.1	12.6	3.5
FeatGen[33]	43.9	9.8	36.2	8.7	34.1	7.4	21.3	5.6
CIZSL[8]	44.6	14.4	36.6	9.3	39.2	11.9	24.5	6.4
CANZSL[64]	45.8	14.3	38.1	8.9	40.2	12.5	25.6	6.8
GDAN[36]	44.2	13.7	38.3	8.7	38.7	10.9	24.1	5.9
Baseline18 [6]	43.7	10.3	35.6	8.6	35.4	8.7	20.4	5.8
CKL-TR[31]	45.8	15.1	36.8	10.0	40.2	12.2	22.3	7.8
MKFNet-NFG	47.5 +3.8	15.9 +5.6	37.4+1.8	12.1 +3.5	40.5 +5.1	14.4 +5.7	23.2+2.8	8.5 +2.7

TABLE III

RESULTS OF COMPARISON WITH STATE-OF-THE-ARTS METHODS IN GENERALIZED ZSL (GZSL) SCENARIO ON FOUR CLASSIFICATION BENCHMARKS. *U* AND *S* ARE THE TOP-1 ACCURACIES TESTED ON UNSEEN CLASSES AND SEEN CLASSES, RESPECTIVELY, IN GZSL. *H* IS THE HARMONIC MEAN OF *U* AND *S*.

methods	CUB-Att			AwA1			AwA2			FLO			aPY		
	<i>U</i>	<i>S</i>	<i>H</i>												
Baseline18 [6]	31.7	61.3	41.8	29.6	84.2	43.8	35.4	86.9	50.3	28.1	77.4	41.2	14.2	78.6	24.0
CLSWGAN [33]	43.7	57.7	49.7	57.9	61.4	59.6	56.1	65.5	60.4	59.0	73.9	65.6	-	-	-
SE-ZSL [34]	41.5	53.3	46.7	56.3	67.8	61.5	58.3	68.1	62.8	-	-	-	-	-	-
LisGAN [66]	46.5	57.9	51.6	52.6	76.3	62.3	47.0	77.6	58.5	57.7	83.8	68.3	-	-	-
f-VAEGAN-D2 [65]	48.4	60.1	53.6	57.6	70.6	63.5	-	-	-	56.8	74.9	64.6	-	-	-
CADA-VAE [67]	51.6	53.5	52.4	57.3	72.8	64.1	55.8	75.0	63.9	-	-	-	31.5	57.1	40.6
RELATION NET [68]	38.1	61.1	47.0	31.4	91.3	46.7	30.0	93.4	45.3	50.8	88.5	64.5	-	-	-
GDAN [36]	39.3	66.7	49.5	-	-	-	32.1	67.5	43.5	-	-	-	30.4	75.0	43.4
DAZLE [15]	56.7	59.6	58.1	-	-	-	60.3	75.0	67.1	-	-	-	-	-	-
RFF-GZSL [35]	50.6	79.1	61.7	59.5	91.6	72.1	-	-	-	61.3	88.8	72.5	-	-	-
OCD [69]	53.2	60.2	56.5	-	-	-	59.5	73.4	65.7	-	-	-	-	-	-
DVBE [12]	53.2	60.2	56.5	-	-	-	63.6	70.8	67.0	-	-	-	32.6	58.3	41.8
ASPNet [70]	50.7	61.5	55.6	58.0	85.7	69.2	46.2	87.0	60.4	67.3	87.4	76.0	-	-	-
APNet [25]	55.9	48.1	51.7	76.6	59.7	67.1	54.8	83.9	66.4	-	-	-	32.7	74.7	45.5
CKL-TR [31]	57.8	50.2	53.7	61.4	93.2	74.0	61.2	92.6	73.7	-	-	-	30.8	78.9	44.3
MKFNet-NFG	58.9	64.8	61.7	65.0	92.9	76.4	61.9	92.2	74.0	76.6	92.4	83.7	30.2	94.0	45.7

space, and the fusion of visual features of higher knowledge level is beneficial to alleviate this phenomenon and expand the class spacing. In addition, the base version MKFNet-base of MKFNet outperforming CKL-TR in some metrics can also illustrate the effectiveness of the proposed model. For example, the *H* metric is improved from 53.7% to 58.7% and 74.0% to 75.2% on CUB-Att and AwA1 datasets, respectively. Although the *H* metric on the aPY dataset has decreased slightly, from 44.3% to 42.8%, MKFNet-base retains a high accuracy in seen classes, increasing from 78.9% to 90.6%. Furthermore, compared with MKFNet, MKFNet-NFG achieved consistent improvements, with *H* metric ranging from 60.0% to 61.7%, 75.4% to 76.4%, and 44.9% to 45.7% on the CUB-Att, AwA1 and aPY datasets, which shows that the NFG method does enable the model to learn some new discriminative features. In general, the overall trend in Table.IV can be observed that with the combination of each component, the performance has been consistently improved. This obviously shows the effectiveness of each component.

TABLE IV

THE INFLUENCE OF DIFFERENT COMPONENTS ON GZSL RESULTS. MKFNET-BASE IS THE BASE VERSION OF MKFNET, WHICH USES SIMPLE SUMMING OPERATION INSTEAD OF THE ADAPTIVE FUSION MODULE OF MKFNET. MKFNET AND MKFNET-NFG REPRESENT USING NFG METHOD AND NOT USING NFG METHOD, RESPECTIVELY.

methods	CUB-Att			AwA1			aPY		
	<i>U</i>	<i>S</i>	<i>H</i>	<i>U</i>	<i>S</i>	<i>H</i>	<i>U</i>	<i>S</i>	<i>H</i>
CKL-TR	57.8	50.2	53.7	61.4	93.2	74.0	30.8	78.9	44.3
MKFNet-base	52.2	67.1	58.7	63.3	92.5	75.2	28.0	90.6	42.8
MKFNet	56.8	63.6	60.0	63.6	92.6	75.4	29.8	90.7	44.9
MKFNet-NFG	58.9	64.8	61.7	65.0	92.9	76.4	30.2	94.0	45.7

D. Visualization Results

Feature Visualization: To investigate the difference between the real visual features and the synthesized visual features of the unseen classes, we visualize the real visual features and synthesized visual features by using t-SNE method and

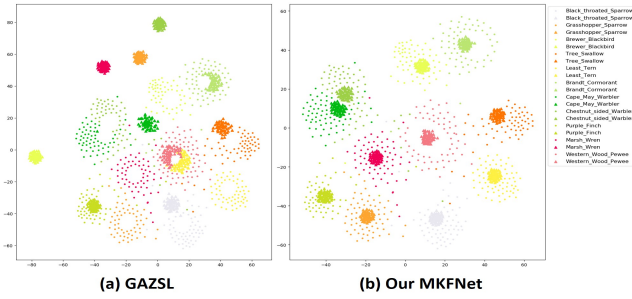


Fig. 5. The t-SNE visualization of real and synthesized visual features. The circle and triangle represents the real visual features and the synthesized visual features, respectively. The different colors represent different classes.

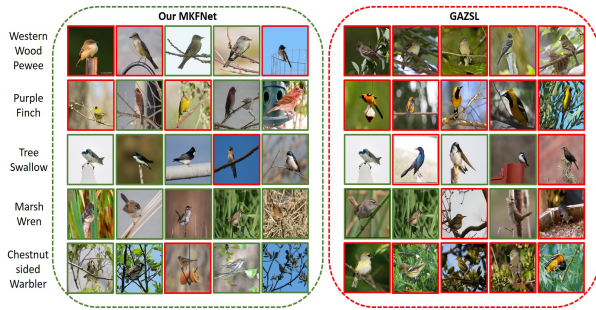


Fig. 6. The ZSL retrieval results of the proposed method in CUB dataset. Each row contains the Top-5 retrieved images of a specific class. The image with a green box and a red box represent correct and wrong retrieval, respectively.

compare the visualization result of the proposed approach with GAZSL [6] on CUB dataset. Specially, for each unseen class on CUB, we use our method and GAZSL to synthesize 60 visual features. The visualization results of GAZSL and ours are shown in Fig.5(a) and Fig.5(b), respectively. As shown in Fig.5(a), there are serious differences in the visual feature distribution between real samples and synthesized samples, especially Marsh Wren, Grasshopper Sparrow and Cape May Warbler et al. In Fig.5(b), it is obviously that the synthesized visual features of our method follow the distribution of the real visual features. This proves that the proposed method can learn more general knowledge and deviate to the unseen class.

Result of ZSL Image Retrieval: We compare the proposed approach with GAZSL [6] on the image retrieval task on CUB. For each semantic feature in CUB, we generate 60 visual features and calculate the visual center point. According to these visual central points, the cosine similarity is calculated with the true visual features, and the Top-5 samples with the highest similarity are selected as the retrieved images. The retrieval results are shown in Fig.6. The green box and red box represent the correct retrieval image and the wrong retrieval image, respectively. The retrieval results show that the proposed approach is more accurate than GAZSL, demonstrating that our approach can learn more discriminative feature and generate more appropriate synthesized visual features.

E. Discuss

In the previous experiments, we used a large number of datasets to indirectly prove that the proposed method achieved

very promising performance. To further discuss why the proposed method is effective, we conducted two additional experiments.

Effectiveness of Adaptive Fusion Module in MKFNet. In this work, we proposed Multi-Knowledge Fusion Network (MKFNet) with adaptive fusion module to meet the domain-shift challenge. The idea of MKFNet is to fuse multiple semantic features from different knowledge. Different knowledge have different universality and specificity. Their fusion can make the generated samples have stronger generalization ability. In order to explore the effectiveness of each knowledge in different benchmarks, we visualize the importance weights of different knowledge domains, as shown in Fig.7. Each subgraph in Fig.7 shows the importance weight of FLO, AWA1 and APY datasets in different knowledge domains. In order to display more information, we select 30 samples from unseen classes randomly and input them into MKFNet, and record the importance weight of different knowledge in each sample. The horizontal axis of each subgraph represents different knowledge (Species, Genus, and Family), and the vertical axis represents the importance weights of 30 samples. Obviously, we can observe that in different datasets, the importance weights of different knowledge domains are all greater than zero. This shows that different knowledge domains have played a role, and further proves the effectiveness of the adaptive fusion module in MKFNet. By introducing higher-level knowledge, we can generate more generalized samples to alleviate the domain-shift problem.

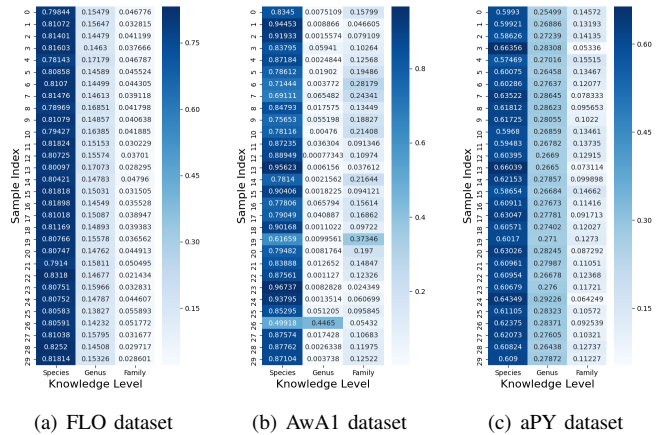


Fig. 7. The importance weight of each knowledge in different benchmarks.

Effectiveness of New Feature Generator in MKFNet. In order to further prove the positive impact of the New Feature Generator (NFG) on the classification of each unseen category, we counted the number of correct classifications for each category on AwA1, AwA2, CUB-Att and FLO datasets. As shown in each sub-graph in the Fig.8, the x-axis represents the name of the unseen category, and the y-axis represents the number of samples correctly classified as the unseen category. An obvious trend is to use NFG's MKFNet to be able to identify more unseen samples. Especially for the AwA1 and AwA2 datasets, MKFNet-NFG has a higher recognition rate than MKFNet on almost every unseen category. This

phenomenon shows that NFG can generate new discriminative features for model learning to synthesize generalized visual features.

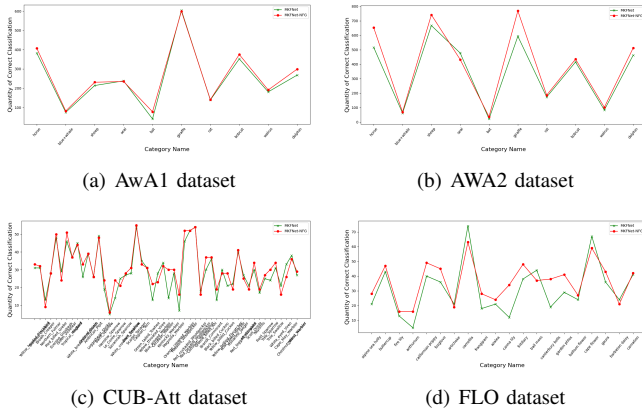


Fig. 8. The influence of using NFG method (MKFNet-NFG) and not using NFG method (MKFNet) on the number of unseen classes correctly identified.

V. CONCLUSION

In this paper, we proposed a novel generative zero-shot learning approach to address the problems of semantic insufficiency and domain-shift problems in ZSL, where Multi-Knowledge Fusion Network (MKFNet) and L_{ER} in New Feature Generator (NFG) are proposed to enhance semantic features by using cross-concept knowledge, and L_{NR} in AGS and L_{KR} are proposed improves the intersection of synthesized visual features and unseen visual features. The experiment results demonstrate that our approach is superior to baselines and several state-of-the-art methods.

ACKNOWLEDGEMENT

This work was supported in part by the Natural Science Foundation of China (NSFC) under Grant 61876166 and Grant 61663046, in part by the Yunnan Applied Fundamental Research Project under Grant 2016FB104, in part by the Yunnan Provincial Young Academic and Technical Leaders Reserve Talents under Grant 2017HB005, in part by the Program for Yunnan High Level Overseas Talent Recruitment, and in part by the Program for Excellent Young Talents of Yunnan University.

REFERENCES

- [1] K. He, X. Zhang, S. Ren, and J. Sun, “Deep residual learning for image recognition,” in *Proceedings of the IEEE conference on computer vision and pattern recognition*, 2016, pp. 770–778. I, IV-A, IV-A
- [2] S. Ren, K. He, R. Girshick, and J. Sun, “Faster r-cnn: Towards real-time object detection with region proposal networks,” *IEEE Transactions on Pattern Analysis & Machine Intelligence*, vol. 39, no. 6, pp. 1137–1149, 2017. I
- [3] X. Sun, H. Xv, J. Dong, H. Zhou, and Q. Li, “Few-shot learning for domain-specific fine-grained image classification,” *IEEE Transactions on Industrial Electronics*, vol. PP, no. 99, pp. 1–1, 2020. I
- [4] W. L. Chao, S. Changpinyo, B. Gong, and F. Sha, “An empirical study and analysis of generalized zero-shot learning for object recognition in the wild,” *Frontiers of Information Technology & Electronic Engineering*, vol. 17, no. 5, pp. 403–412, 2016. I, IV-A

- [5] M. Elhoseiny, Y. Zhu, H. Zhang, and A. Elgammal, “Link the head to the beak”: Zero shot learning from noisy text description at part precision,” in *2017 IEEE Conference on Computer Vision and Pattern Recognition (CVPR)*. IEEE, 2017, pp. 6288–6297. I, IV-A, IV-A
- [6] Y. Zhu, M. Elhoseiny, B. Liu, X. Peng, and A. Elgammal, “A generative adversarial approach for zero-shot learning from noisy texts,” in *Proceedings of the IEEE conference on computer vision and pattern recognition*, 2018, pp. 1004–1013. I, I, II-A, II-A, III-A, III-B, IV-A, IV-A, IV-A, IV-A, IV-B, II, III, IV-D, IV-D
- [7] Y. Xian, C. H. Lampert, B. Schiele, and Z. Akata, “Zero-shot learning—a comprehensive evaluation of the good, the bad and the ugly,” *IEEE transactions on pattern analysis and machine intelligence*, vol. 41, no. 9, pp. 2251–2265, 2018. I, IV-A
- [8] M. Elhoseiny and M. Elfeki, “Creativity inspired zero-shot learning,” in *Proceedings of the IEEE International Conference on Computer Vision*, 2019, pp. 5784–5793. I, I, IV-A, IV-A, IV-A, IV-A, II
- [9] J. Weston, S. Bengio, and N. Usunier, “Large scale image annotation: learning to rank with joint word-image embeddings,” *Machine learning*, vol. 81, no. 1, pp. 21–35, 2010. I
- [10] Z. Akata, F. Perronnin, Z. Harchaoui, and C. Schmid, “Label-embedding for attribute-based classification,” in *Proceedings of the IEEE Conference on Computer Vision and Pattern Recognition*, 2013, pp. 819–826. I
- [11] Z. Ji, K. Chen, J. Wang, Y. Yu, and Z. Zhang, “Multi-modal generative adversarial network for zero-shot learning,” *Knowledge-Based Systems*, vol. 197, p. 105847, 2020. I
- [12] S. Min, H. Yao, H. Xie, C. Wang, Z.-J. Zha, and Y. Zhang, “Domain-aware visual bias eliminating for generalized zero-shot learning,” in *Proceedings of the IEEE/CVF Conference on Computer Vision and Pattern Recognition*, 2020, pp. 12 664–12 673. I, IV-A, III
- [13] P. Zhu, H. Wang, and V. Saligrama, “Generalized zero-shot recognition based on visually semantic embedding,” in *Proceedings of the IEEE Conference on Computer Vision and Pattern Recognition*, 2019, pp. 2995–3003. I
- [14] G.-S. Xie, L. Liu, X. Jin, F. Zhu, and L. Shao, “Attentive region embedding network for zero-shot learning,” in *2019 IEEE/CVF Conference on Computer Vision and Pattern Recognition (CVPR)*, 2020. I
- [15] D. Huynh and E. Elhamifar, “Fine-grained generalized zero-shot learning via dense attribute-based attention,” in *Proceedings of the IEEE/CVF Conference on Computer Vision and Pattern Recognition*, 2020, pp. 4483–4493. I, II-B, II-B, III
- [16] S. Liu, J. Chen, L. Pan, C.-W. Ngo, T.-S. Chua, and Y.-G. Jiang, “Hyperbolic visual embedding learning for zero-shot recognition,” in *Proceedings of the IEEE/CVF Conference on Computer Vision and Pattern Recognition*, 2020, pp. 9273–9281. I
- [17] Z. Akata, S. Reed, D. Walter, H. Lee, and B. Schiele, “Evaluation of output embeddings for fine-grained image classification,” in *Proceedings of the IEEE conference on computer vision and pattern recognition*, 2015, pp. 2927–2936. I
- [18] Z. Fu, T. Xiang, E. Kodirov, and S. Gong, “Zero-shot object recognition by semantic manifold distance,” in *Proceedings of the IEEE conference on computer vision and pattern recognition*, 2015, pp. 2635–2644. I
- [19] G.-J. Qi, W. Liu, C. Aggarwal, and T. Huang, “Joint intermodal and intramodal label transfers for extremely rare or unseen classes,” *IEEE transactions on pattern analysis and machine intelligence*, vol. 39, no. 7, pp. 1360–1373, 2016. I
- [20] Y. Zhu, J. Xie, Z. Tang, X. Peng, and A. Elgammal, “Semantic-guided multi-attention localization for zero-shot learning,” in *Advances in Neural Information Processing Systems*, 2019, pp. 14 943–14 953. I, II-B, II-B
- [21] Z. Ji, Y. Fu, J. Guo, Y. Pang, Z. M. Zhang *et al.*, “Stacked semantics-guided attention model for fine-grained zero-shot learning,” in *Advances in Neural Information Processing Systems*, 2018, pp. 5995–6004. I, II-B
- [22] Y. Liu, J. Guo, D. Cai, and X. He, “Attribute attention for semantic disambiguation in zero-shot learning,” in *Proceedings of the IEEE International Conference on Computer Vision*, 2019, pp. 6698–6707. I, II-B
- [23] M. Kampffmeyer, Y. Chen, X. Liang, H. Wang, Y. Zhang, and E. P. Xing, “Rethinking knowledge graph propagation for zero-shot learning,” in *Proceedings of the IEEE Conference on Computer Vision and Pattern Recognition*, 2019, pp. 11 487–11 496. I, II-A
- [24] C.-W. Lee, W. Fang, C.-K. Yeh, and Y.-C. Frank Wang, “Multi-label zero-shot learning with structured knowledge graphs,” in *Proceedings of the IEEE conference on computer vision and pattern recognition*, 2018, pp. 1576–1585. I

- [25] L. Liu, T. Zhou, G. Long, J. Jiang, and C. Zhang, "Attribute propagation network for graph zero-shot learning," in *AAAI*, 2020, pp. 4868–4875. I, II-A, III
- [26] Y. Fu, T. M. Hospedales, T. Xiang, and S. Gong, "Transductive multi-view zero-shot learning," *IEEE transactions on pattern analysis and machine intelligence*, vol. 37, no. 11, pp. 2332–2345, 2015. I
- [27] Y. Fu, T. M. Hospedales, T. Xiang, and S. Gong, "Transductive multi-view zero-shot learning," *IEEE Transactions on Pattern Analysis and Machine Intelligence*, vol. 37, no. 11, pp. 2332–2345, 2015. I
- [28] Y. Fu, T. Hospedales, T. Xiang, and S. Gong, "Transductive multi-view zero-shot learning," *IEEE Transactions on Pattern Analysis and Machine Intelligence*, vol. 37, 01 2015. I
- [29] Y. Guo, G. Ding, X. Jin, and J. Wang, "Transductive zero-shot recognition via shared model space learning," in *Thirtieth AAAI Conference on Artificial Intelligence*, 2016. I
- [30] Y. Yu, Z. Ji, J. Guo, and Y. Pang, "Transductive zero-shot learning with adaptive structural embedding," *IEEE Transactions on Neural Networks and Learning Systems*, vol. 29, no. 9, pp. 4116–4127, 2018. I
- [31] C. Xie, H. Xiang, T. Zeng, Y. Yang, B. Yu, and Q. Liu, "Cross knowledge-based generative zero-shot learning approach with taxonomy regularization," 2021. I, III-A, III-B, III-B, IV-C, II, III
- [32] Y. Long, L. Liu, L. Shao, F. Shen, G. Ding, and J. Han, "From zero-shot learning to conventional supervised classification: Unseen visual data synthesis," in *Proceedings of the IEEE Conference on Computer Vision and Pattern Recognition*, 2017, pp. 1627–1636. II-A, II-A
- [33] Y. Xian, T. Lorenz, B. Schiele, and Z. Akata, "Feature generating networks for zero-shot learning," in *Proceedings of the IEEE conference on computer vision and pattern recognition*, 2018, pp. 5542–5551. II-A, II-A, IV-A, IV-A, IV-B, II, III
- [34] V. Kumar Verma, G. Arora, A. Mishra, and P. Rai, "Generalized zero-shot learning via synthesized examples," in *Proceedings of the IEEE conference on computer vision and pattern recognition*, 2018, pp. 4281–4289. II-A, II-A, III
- [35] Z. Han, Z. Fu, and J. Yang, "Learning the redundancy-free features for generalized zero-shot object recognition," in *Proceedings of the IEEE/CVF Conference on Computer Vision and Pattern Recognition*, 2020, pp. 12865–12874. II-A, II-A, IV-A, III
- [36] H. Huang, C. Wang, P. S. Yu, and C.-D. Wang, "Generative dual adversarial network for generalized zero-shot learning," in *Proceedings of the IEEE/CVF Conference on Computer Vision and Pattern Recognition (CVPR)*, June 2019. II-A, IV-B, II, III
- [37] F. Wang, M. Jiang, C. Qian, S. Yang, C. Li, H. Zhang, X. Wang, and X. Tang, "Residual attention network for image classification," in *Proceedings of the IEEE conference on computer vision and pattern recognition*, 2017, pp. 3156–3164. II-B, III-C
- [38] H. Guo, K. Zheng, X. Fan, H. Yu, and S. Wang, "Visual attention consistency under image transforms for multi-label image classification," in *Proceedings of the IEEE Conference on Computer Vision and Pattern Recognition*, 2019, pp. 729–739. II-B, III-C
- [39] L.-C. Chen, Y. Yang, J. Wang, H. Xu, and A. L. Yuille, "Attention to scale: Scale-aware semantic image segmentation," in *Proceedings of the IEEE conference on computer vision and pattern recognition*, 2016, pp. 3640–3649. II-B
- [40] D. Nie, Y. Gao, L. Wang, and D. Shen, "Asdnet: Attention based semi-supervised deep networks for medical image segmentation," in *International Conference on Medical Image Computing and Computer-Assisted Intervention*. Springer, 2018, pp. 370–378. II-B
- [41] T. Xu, P. Zhang, Q. Huang, H. Zhang, Z. Gan, X. Huang, and X. He, "Attngan: Fine-grained text to image generation with attentional generative adversarial networks," in *Proceedings of the IEEE conference on computer vision and pattern recognition*, 2018, pp. 1316–1324. II-B
- [42] L. Gao, D. Chen, Z. Zhao, J. Shao, and H. T. Shen, "Lightweight dynamic conditional gan with pyramid attention for text-to-image synthesis," *Pattern Recognition*, p. 107384, 2020. II-B
- [43] Y. Sun, B. Xue, M. Zhang, G. G. Yen, and J. Lv, "Automatically designing cnn architectures using the genetic algorithm for image classification," *IEEE Transactions on Cybernetics*, vol. PP, no. 99, pp. 1–15, 2020. II-C, II-C
- [44] B. Ma, X. Li, Y. Xia, and Y. Zhang, "Autonomous deep learning: A genetic dcnn designer for image classification," *Neurocomputing*, vol. 379, no. Feb.28, pp. 152–161, 2020. II-C, II-C
- [45] Z. Li, H. Ma, D. Li, and R. Fan, "Genetic algorithm optimization of convolutional neural network for liver cancer ct image classification," in *2018 IEEE 4th Information Technology and Mechatronics Engineering Conference (ITOEC)*, 2018. II-C
- [46] Z. Ye, A. Zhang, Y. Cao, L. Ma, C. Jin, X. Hu, and J. Hu, "An image thresholding method based on differential evolution algorithm and genetic algorithm," in *2019 10th IEEE International Conference on Intelligent Data Acquisition and Advanced Computing Systems: Technology and Applications (IDAACS)*, 2019. II-C
- [47] I. Gulrajani, F. Ahmed, M. Arjovsky, V. Dumoulin, and A. C. Courville, "Improved training of wasserstein gans," in *NIPS*, 2017, pp. 5767–5777. III-B
- [48] A. Odena, C. Olah, and J. Shlens, "Conditional image synthesis with auxiliary classifier gans," pp. 2642–2651, 2017. III-B
- [49] P. Welinder, S. Branson, T. Mita, C. Wah, F. Schroff, S. Belongie, and P. Perona, "Caltech-ucsd birds 200," 09 2010. IV-A, IV-A
- [50] G. V. Horn, S. Branson, R. Farrell, S. Haber, and S. Belongie, "Building a bird recognition app and large scale dataset with citizen scientists: The fine print in fine-grained dataset collection," in *2015 IEEE Conference on Computer Vision and Pattern Recognition (CVPR)*, 2015. IV-A
- [51] M.-E. Nilsback and A. Zisserman, "Automated flower classification over a large number of classes," in *2008 Sixth Indian Conference on Computer Vision, Graphics & Image Processing*. IEEE, 2008, pp. 722–729. IV-A, IV-A
- [52] C. H. Lampert, H. Nickisch, and S. Harmeling, "Learning to detect unseen object classes by between-class attribute transfer," in *2009 IEEE Conference on Computer Vision and Pattern Recognition*. IEEE, 2009, pp. 951–958. IV-A
- [53] Y. Xian, C. H. Lampert, B. Schiele, and Z. Akata, "Zero-shot learning—a comprehensive evaluation of the good, the bad and the ugly," *IEEE Transactions on Pattern Analysis and Machine Intelligence*, vol. 41, pp. 2251–2265, 2017. IV-A, IV-A, IV-A, IV-A
- [54] A. Farhadi, I. Endres, D. Hoiem, and D. Forsyth, "Describing objects by their attributes," in *IEEE Conference on Computer Vision & Pattern Recognition*, 2009, pp. 1778–1785. IV-A
- [55] S. Reed, Z. Akata, H. Lee, and B. Schiele, "Learning deep representations of fine-grained visual descriptions," in *Proceedings of the IEEE Conference on Computer Vision and Pattern Recognition*, 2016, pp. 49–58. IV-A, IV-A
- [56] Y. Yu, Z. Ji, J. Han, and Z. Zhang, "Episode-based prototype generating network for zero-shot learning," in *Proceedings of the IEEE/CVF Conference on Computer Vision and Pattern Recognition*, 2020, pp. 14035–14044. IV-A
- [57] L. Zhang, T. Xiang, and S. Gong, "Learning a deep embedding model for zero-shot learning," in *Proceedings of the IEEE Conference on Computer Vision and Pattern Recognition*, 2017, pp. 2021–2030. IV-A
- [58] M. Elhoseiny, "Write a classifier: Zero shot learning using purely textual descriptions," 12 2013. II
- [59] M. Elhoseiny, A. Elgammal, and B. Saleh, "Write a classifier: Predicting visual classifiers from unstructured text," *IEEE Transactions on Pattern Analysis and Machine Intelligence*, vol. 39, no. 12, pp. 2539–2553, 2017. II
- [60] B. Romera-Paredes and P. H. S. Torr, "An embarrassingly simple approach to zero-shot learning," in *Proceedings of the 32nd international conference on Machine learning (ICML '15)*, 2015. II
- [61] R. Qiao, L. Liu, C. Shen, and A. Hengel, "Less is more: zero-shot learning from online textual documents with noise suppression," 04 2016. II
- [62] S. Changpinyo, W. L. Chao, B. Gong, and F. Sha, "Synthesized classifiers for zero-shot learning," in *2016 IEEE Conference on Computer Vision and Pattern Recognition (CVPR)*, 2016. II
- [63] M. Elhoseiny, Y. Zhu, H. Zhang, and A. Elgammal, "Link the head to the "beak": Zero shot learning from noisy text description at part precision," 07 2017. II
- [64] Z. Chen, J. Li, Y. Luo, Z. Huang, and Y. Yang, "Canzsl: Cycle-consistent adversarial networks for zero-shot learning from natural language," in *The IEEE Winter Conference on Applications of Computer Vision*, 2020, pp. 874–883. II
- [65] Y. Xian, S. Sharma, B. Schiele, and Z. Akata, "f-vaegan-d2: A feature generating framework for any-shot learning," in *Proceedings of the IEEE Conference on Computer Vision and Pattern Recognition*, 2019, pp. 10275–10284. IV-B, III
- [66] J. Li, M. Jing, K. Lu, Z. Ding, L. Zhu, and Z. Huang, "Leveraging the invariant side of generative zero-shot learning," in *Proceedings of the IEEE Conference on Computer Vision and Pattern Recognition*, 2019, pp. 7402–7411. IV-B, III
- [67] E. Schonfeld, S. Ebrahimi, S. Sinha, T. Darrell, and Z. Akata, "Generalized zero-and few-shot learning via aligned variational autoencoders," in *Proceedings of the IEEE Conference on Computer Vision and Pattern Recognition*, 2019, pp. 8247–8255. III
- [68] F. Sung, Y. Yang, L. Zhang, T. Xiang, P. H. Torr, and T. M. Hospedales, "Learning to compare: Relation network for few-shot learning," in

Proceedings of the IEEE Conference on Computer Vision and Pattern Recognition, 2018, pp. 1199–1208. III

- [69] R. Keshari, R. Singh, and M. Vatsa, “Generalized zero-shot learning via over-complete distribution,” in *Proceedings of the IEEE/CVF Conference on Computer Vision and Pattern Recognition*, 2020, pp. 13 300–13 308. III
- [70] Z. Lu, Y. Yu, Z.-M. Lu, F.-L. Shen, and Z. Zhang, “Attentive semantic preservation network for zero-shot learning,” in *Proceedings of the IEEE/CVF Conference on Computer Vision and Pattern Recognition Workshops*, 2020, pp. 682–683. III